Check for updates

Catalytic dinitrogen reduction to hydrazine and ammonia using Cr(N₂)₂(diphosphine)₂ complexes†

Charles H. Beasley, [ID] [a] Olivia L. Duletski, [ID] [a] Ksenia S. Stankevich, [ID] [a] Navamoney Arulsamy [ID] [b] and Michael T. Mock [ID] *[a]

The synthesis, characterization of *trans*-[Cr(N_2)₂(depe)₂] (**1**) is described. **1** and *trans*-[Cr(N_2)₂(dmpe)₂] (**2**) catalyze the reduction of N_2 to N_2H_4 and NH_3 in THF using SmI_2 and H_2O or ethylene glycol as proton sources. **2** produces the highest total fixed N for a molecular Cr catalyst to date.

Motivated by the desire to understand and control the challenging multi-proton, multi-electron reaction of N_2 reduction to NH_3, researchers have intensely studied the reactivity of molecular transition metal dinitrogen complexes.[1] Well-defined molecular systems offer a high degree of electronic and structural control to regulate chemical reactivity of N_2.[2] When combined with effective strategies to form N–H bonds, such as proton-coupled electron transfer (PCET) reagents,[3] *i.e.* SmI_2 and a proton source, tens-of-thousands of equivalents of NH_3 can be generated.[4] The valuable information obtained from these studies includes the identification of viable M–N_xH_y reaction intermediates from spectroscopic data that can be used to delineate the mechanistic steps of a putative catalytic cycle. Such studies can aid in the understanding of the mechanistically complex biological N_2 fixation processes carried out by nitrogenase enzymes,[5] as well as heterogeneous Haber–Bosch catalysts.[6]

Group 6 N_2 complexes bearing monodentate phosphine ligands, especially with Mo and W, were among the first molecular systems to generate stoichiometric quantities of N_2-derived NH_3 from protonolysis reactions with strong acids nearly 50 years ago.[7] Recently, a renaissance of examining structurally similar [M(N_2)₂(P–P)₂], (M = Mo, W; P–P = diphosphine) systems has begun, elevating these simple complexes as catalysts for N_2 reduction to NH_3, or other remarkable reactions such as cleavage of the N_2 triple bond.[8] Masuda and co-workers reported spontaneous N≡N bond cleavage upon one-electron oxidation of *trans*-[Mo(N_2)₂(depe)₂] (depe = $Et_2PCH_2CH_2PEt_2$) to form [Mo(N)(depe)₂]⁺.[9] Chirik and co-workers developed a photocatalytic strategy to form NH_3 from [Mo(N)(depe)₂]⁺ and H_2.[10] Electrocatalytic N_2 fixation with Mo and W-phosphine complexes was described by Peters and co-workers using a tandem catalysis approach.[11] Nishibayashi and co-workers showed simple Mo-phosphine complexes catalyzed N_2 reduction to NH_3 using SmI_2 and various proton sources.[12]

While these examples highlight new discoveries using [M(N_2)₂(P–P)₂] (M = Mo, W) complexes, catalytic N_2 reduction with analogous Cr compounds are limited. Recent reports highlighted the utility of molecular Cr complexes using a variety of ligand architectures for N_2 activation,[8a,13] functionalization,[14] or catalytic N_2 silylation.[15] However, molecular Cr complexes that catalyze the direct reduction of N_2 to NH_3 are rare. In 2022, Nishibayashi and co-workers reported a Cr complex bearing a PCP pincer ligand that catalyzed direct N_2 reduction to NH_3 and N_2H_4 at −78 °C to rt. KC_8 and phosphonium salts as H⁺ sources were required for turnover, and this system was not catalytic using SmI_2.[16] Herein we prepared and characterized *trans*-[Cr(N_2)₂(depe)₂] (**1**), and report catalytic N_2 reduction to NH_3 and N_2H_4 with **1** and *trans*-[Cr(N_2)₂(dmpe)₂][17] (**2**) (dmpe = $Me_2PCH_2CH_2PMe_2$) at room temperature using SmI_2 and ethylene glycol or H_2O as proton sources.

Vigorous stirring of yellow *trans*-[CrCl₂(depe)₂][18] (**1-Cl**) in THF with excess Mg powder under a N_2 atmosphere for 24 h furnished **1** as a dark red solid in 70% yield. Isolation of **1** allowed for a comparison of the structural and spectroscopic data with **2** that was reported in 1983.[17a] The structure of **1**, determined by single crystal X-ray diffraction, shows Cr with four phosphorus atoms of the chelates on the equatorial plane and two axial end-on bound N_2 ligands, Fig. 1, panel a. The average Cr–N, Cr–P, and N≡N bond distances are 1.904 ± 0.005 Å, 2.334 ± 0.007 Å, and 1.104 ± 0.004 Å, respectively. The corresponding Cr–N, and Cr–P, bond distances in **2** (see ESI†),

aDepartment of Chemistry and Biochemistry, Montana State University, Bozeman, MT 59717, USA. E-mail: michael.mock@montana.edu
bDepartment of Chemistry, University of Wyoming, Laramie, WY, 82071, USA
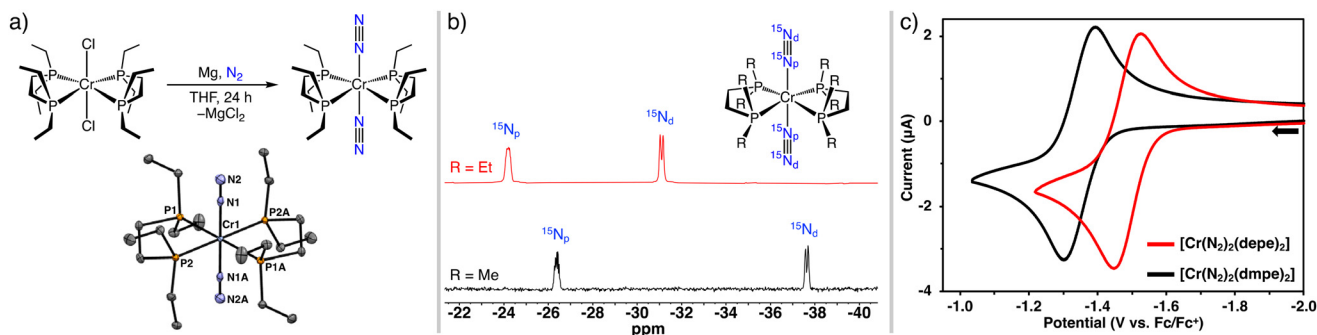
Fig. 1 (a) Synthesis and molecular structure of **1**. Thermal ellipsoids are drawn at 50% probability. Hydrogen atoms are omitted for clarity. Crystals of **1** contain two molecules per asymmetric unit with comparable metric parameters; only one molecule is shown. Selected bond distances (Å) and angles (°): Cr1–N1 = 1.9081(10); N1–N2 = 1.1003(14); Cr–P1 = 2.3343(3); Cr–P2 = 2.3249(3). Cr2–N3 = 1.9008(10); N3–N4 = 1.1069(14); Cr–P3 = 2.3425(3); Cr–P4 = 2.3346(3). P1–Cr1–P2 = 81.650(9); P3–Cr2–P4 = 81.583(10); P1–Cr1–N1 = 89.25(3); P2–Cr1–N1 = 90.21(3); P3–Cr2–N3 = 89.29(3); P4–Cr2–N3 = 90.59(3). (b) $^{15}N\{^1H\}$ NMR spectra of 1^{15N} (red) and 2^{15N} (black) recorded at 25 °C in THF-d_8. (c) Cyclic voltammograms of **1** and **2** in THF showing the $Cr^{I/0}$ wave.

are slightly shorter at 1.8862(17) Å, and 2.294 ± 0.005 Å, and the N≡N distance is 1.110(2) Å.[19] The ligand bite angles for **1** and **2**, *i.e.* P1–Cr–P2, are 81.6° and 83.5°, respectively, and the P–Cr–N angles are near 90°.

The $^{31}P\{^1H\}$ NMR spectrum of **1** in THF-d_8, displays a singlet at 79.9 ppm (68.8 ppm for **2**) consistent with four magnetically equivalent P atoms. Complexes **1** and **2** were characterized by ^{15}N NMR spectroscopy to augment the cumulative library of tabulated ^{15}N NMR data of phosphine-supported group 6 N_2 complexes.[13h] The $^{15}N_2$-labelled complexes 1^{15N} and 2^{15N}, were prepared by mixing the respective Cr–N_2 complexes in THF-d_8 under 1 atm $^{15}N_2$. The ^{15}N NMR spectra were collected after mixing for 24 h. The $^{15}N\{^1H\}$ NMR spectra contain two resonances; a doublet (J_{NN} = 7.0 Hz) and a multiplet (~2.5 Hz ^{31}P coupling) (1^{15N}: –31.1 ppm, –24.2 ppm, and 2^{15N}: –37.6 ppm, –26.4 ppm), assigned as the distal (N_d) and proximal (N_p) nitrogen atoms, respectively, (Fig. 1, panel b).[13i]

Cyclic voltammetry (CV) experiments established the redox behaviour of the Cr(0)-N_2 complexes. Voltammograms were recorded using a glassy carbon working electrode at 0.1 V s^{-1} in THF. The voltammogram for each complex displays a reversible, one-electron $Cr^{I/0}$ wave with the half-wave potential ($E_{1/2}$) of –1.49 V and –1.34 V ($vs.$ $Cp_2Fe^{+/0}$) for **1** and **2**, respectively (Fig. 1, panel c). The electrochemically reversible $Cr^{I/0}$ couples indicate N_2 dissociation does not occur upon oxidation to Cr(I) during the CV experiments. The reversibility of the waves for **1** and **2** contrasts other *cis*- or *trans*-[Cr(N$_2$)$_2$(P$_4$)] complexes measured by CV that exhibit quasi-reversible or irreversible $Cr^{I/0}$ waves due to rapid N_2 loss upon oxidation.[13b,c,i] In the current study, an irreversible anodic wave was assigned to the $Cr^{II/I}$ redox feature at E_{pa} = –0.48 V and E_{pa} = –0.63 V, for **1** and **2**, respectively, due to N_2 dissociation at more positive potentials, (Fig. S17 and S18 ESI†). The CV results suggest a one-electron chemical oxidation to form *trans*-[Cr(N$_2$)$_2$(P-P)$_2$]$^+$ should be possible; however, our attempts to isolate such a species have been unsuccessful. Owing to the more electron-rich metal centre of **1**, the ν_{NN} band in the infrared spectrum

at 1906 cm^{-1} (THF) appears at lower energy than the ν_{NN} band for **2** at 1917 cm^{-1} (THF).

Complexes **1** and **2** were examined as catalysts for the direct reduction of N_2 to NH_3 and N_2H_4. The catalysis studies were performed in THF at room temperature using the PCET reagent SmI_2 and ethylene glycol and/or water as proton donors. A typical catalytic run used 583 equiv. SmI_2, 1166 equiv. ROH per Cr centre and was stirred for 48 h. Quantification of NH_3, N_2H_4 and H_2 (see ESI for details†) products assessed the total fixed N generated in each reaction. Selected catalytic data are listed in Table 1 (see ESI for all tabulated results†).

Analysis of the catalysis results provides insights about the performance of **1** and **2** under identical reaction conditions. **2** afforded more total fixed N than **1** in all catalytic trials. For example, **1** generated up to 5 equiv. of NH_3 and 5 equiv. N_2H_4 per Cr center using ethylene glycol as the proton donor after >100 h. Under identical conditions, **2** produced up to 16 equiv. NH_3 and 10 equiv. N_2H_4 in 48 h. Furthermore, ethylene glycol worked more effectively as the proton donor affording higher total fixed N than using H_2O. The deleterious effect of H_2O on catalysis was noted in reactions with **2** using ethylene glycol as the primary proton source. As the amount of H_2O added to the reaction increased, NH_3 production declined, while the N_2H_4 formed stayed relatively constant. We postulate the Cr complexes may simply be more prone to degradation in the presence of H_2O. Separately, **2** was treated with 500 equiv. H_2O or ethylene glycol in THF-d_8. Free dmpe from complex degradation appeared more rapidly using H_2O, as assessed by ^{31}P NMR spectroscopy. Catalysis performed with **2** under an atmosphere of $^{15}N_2$ afforded $^{15}NH_4^+$ as a doublet at 7.1 ppm (J_{15N-1H} = 71 Hz) in the ^1H NMR spectrum, identifying $^{15}N_2$ as the source of $^{15}NH_3$.

Catalytic trials using *trans*-[CrCl$_2$(dmpe)$_2$] (**2-Cl**) and ethylene glycol generated comparable amounts of NH_3 and N_2H_4 as using **2** as the precatalyst. **1-Cl** did not catalyze N_2 reduction, affording only 1 equiv. of NH_3 and N_2H_4 per Cr center. SmI_2

Table 1 Selected Cr-catalyzed N_2 reduction experiments

$$N_2 + SmI_2 + ROH \xrightarrow[\text{THF, rt}]{\text{[Cr] cat.}} NH_3 + N_2H_4 + H_2$$

| Entry	Cr cat.	ROH	NH_3 equiv./Cr[a]	N_2H_4 equiv./Cr[b]	Total fixed N	Time (h)
1	None	$(CH_2OH)_2$	0	0	0	48
2	**1**	$(CH_2OH)_2$	3.7 ± 0.9	1.4 ± 0.8	$4.9^h \pm 1.5$	48
3	**1**	$(CH_2OH)_2$	4.6 ± 0.6	4.0 ± 1.7	$8.6^h \pm 2.1$	100
4[c]	**1**	H_2O	1.4	0.7	2.1	48
5[d]	**1**	H_2O	3.2	0.6	3.8	28
6	**1-Cl**	$(CH_2OH)_2$	1.2	0.9	2.1	48
7	**2**	$(CH_2OH)_2$	14.6 ± 1.6	5.9 ± 2.9	$20.5^h \pm 3.8$	48
8[e]	**2**	$(CH_2OH)_2$	6.2 ± 0.5	6.4 ± 0.8	$12.6^h \pm 0.3$	48
9[f]	**2**	$(CH_2OH)_2$	4.4 ± 0.9	6.6 ± 0.6	$11^h \pm 0.4$	48
10[g]	**2**	$(CH_2OH)_2$	1.1	5.7	6.8	48
11[d]	**2**	H_2O	5.1	5.9	11	3
12	**2-Cl**	$(CH_2OH)_2$	13.5 ± 2.8	5.9 ± 0.6	$19.4^h \pm 3.4$	48

Experiments performed using 0.6 μmol catalyst in 15.0 mL THF at 25 °C under 1 atm N_2, with 583 equiv. of SmI_2, and with 1166 equiv. ROH unless otherwise specified. [a] Determined by acidification and NH_4^+ quantification using ^1H NMR spectroscopy (see ESI†). [b] Determined by colorimetric p-dimethylaminobenzaldehyde method (see ESI†). [c] 1000 equiv. H_2O/Cr. [d] 10 000 equiv. H_2O/Cr. [e] 25 ppm of H_2O. [f] 250 ppm of H_2O. [g] 583 equiv. $(CH_2OH)_2$, 583 equiv. H_2O. [h] Average of two or more trials. H_2 quantification by gas chromatography, values are tabulated in ESI.†

and ethylene glycol may be ineffective at reducing the Cr(II) center of **1-Cl** to Cr(0) where N_2 is strongly activated. Treatment of **2-Cl** with 2 equiv. SmI_2 and 2 equiv. ethylene glycol rapidly generated **2** (see ESI†). However, the same reaction of **1-Cl** and SmI_2 with ethylene glycol additive did not form **1** ($E_{1/2} = -1.49$ V, *vide supra*). **1** or **2** could not be generated from **1-Cl** or **2-Cl** using excess $SmI_2(THF)$ alone (E° of $SmI_2(THF) = -1.41 \pm 0.08$ V[20] vs. Fc/Fc^+). A Cr(I) species could be accessible, but N_2 activation and subsequent functionalization steps may be moderated at Cr(I), limiting catalysis.

The mixed N_2 reduction selectivity to form NH_3 and N_2H_4 provides preliminary evidence for a catalytic cycle that follows, at least in part, an alternating N_2 reduction mechanism, Fig. 2, bottom. A purely distal N_2 reduction pathway, Fig. 2, top, would be selective for NH_3 formation. In a 1986 report, the reaction of **2** with CF_3SO_3H was postulated to form a Cr-hydrazido product, $[Cr(NNH_2)(dmpe)_2][CF_3SO_3]_2$.[21] A recent study by Wei, Yi, Xi, and co-workers examining early stage N_2 functionalization of $[Cp*Cr^0(depe)(N_2)]^-$ ($Cp* = \eta^5-C_5(CH_3)_5$) using a variety of electrophiles (H^+, Me_3Si^+, Me^+) also revealed the selective formation of Cr-hydrazido products, consistent

with a distal pathway. Contrary to these reaction patterns, protonation studies of related *cis-* or *trans-*$[Cr(N_2)_2(P_4)]$ complexes we examined using strong acids or H^+/e^- reagents, as well as the catalytic Cr[PCP] system[16] generated NH_3 and N_2H_4.[13c,i,15a] Considering all these examples, and that N_2 reduction mechanisms are sensitive to reaction conditions, (*i.e.* identity of the H^+ and e^- reagents, solvent, temperature), a hybrid N_2 reduction pathway[22] where the third and fourth N–H bonds are formed at the proximal N atom of a Cr-hydrazido intermediate, Fig. 2, middle, cannot be excluded for the current systems. Further studies are warranted to understand the N_2 reduction pathways with Cr.

The proclivity for N_2 ligand substitution in **1** and **2** was evaluated as a metric that could reflect catalyst stability and influence catalytic performance. We examined reactions of **1** and **2** with CO to assess the rate of ligand exchange, Fig. 3. Ligand substitution in these six-coordinate complexes is expected to be a dissociative process; a result of Cr–N or Cr–P bond dissociation. Wilkinson, Hursthouse, and co-workers noted **2** did not react with 7 atm CO for several hours except under u.v. irradiation (in light petroleum) to form *cis-*$[Cr(CO)_2(dmpe)_2]$ (***cis*-2-CO**).[17b] This account was surprising, and the unreactive nature toward N_2/CO exchange seemed uncharacteristic of a
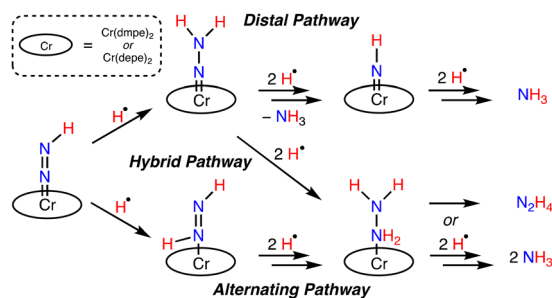
Fig. 2 Plausible N_2 reduction mechanisms for Cr mediated formation of hydrazine and ammonia.
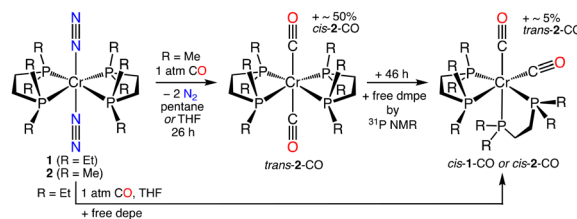
Fig. 3 Ligand exchange reactions of **1** and **2** with CO display different reaction profiles.

complex with terminally bound N_2 ligands. We reacted **2** with 1 atm CO at 25 °C in pentane or THF without u.v. irradiation and monitored the reaction by *in situ* IR spectroscopy, or ^{31}P NMR spectroscopy (see ESI†). In both solvents the reaction was slow, but **2** was not unreactive. In THF, after 26 h ~85% of **2** converted to a ~1:1 mixture of ***cis*-2-CO** and *trans*-[Cr(CO)$_2$(dmpe)$_2$] (***trans*-2-CO**). ***trans*-2-CO** converts to ~95% ***cis*-2-CO** (and ~5% free dmpe) after additional 46 h by ^{31}P NMR spectroscopy. In THF, **1** converts directly to *cis*-[Cr(CO)$_2$(depe)$_2$] ***cis*-1-CO** (ν_{CO} = 1829, 1768 cm^{-1}) in ~3 h by *in situ* IR spectroscopy (see ESI†). The vastly different rates of N_2/CO ligand exchange underscore the greater kinetic stability of **2** toward Cr–L dissociative processes that could ultimately curtail catalyst deactivation pathways (*i.e.* ligand loss) improving catalyst performance for N_2 reduction compared to **1**.

In conclusion, we present a contemporary advancement in the use of *trans*-[Cr(N$_2$)$_2$(P–P)$_2$] complexes (**1** and **2**) for direct catalytic reduction of N_2 to form NH_3 and N_2H_4 using the PCET reagent SmI$_2$ and H$_2$O and/or ethylene glycol as proton donors. A new complex, *trans*-[Cr(N$_2$)$_2$(depe)$_2$], was presented herein. Despite having similar electronic structures, we posit **2** is a better catalyst than **1** (using the presented conditions), due to a less negative Cr$^{I/0}$ redox couple and greater kinetic stability from Cr–L dissociative processes.

Author contributions

C. Beasley, investigation, methodology, writing, editing; O. L. Duletski, investigation; K. S. Stankevich, investigation; N. Arulsamy, investigation, writing; M. T. Mock, conceptualization, methodology, supervision, writing, editing, funding acquisition.

Conflicts of interest

There are no conflicts of interest to declare.

Acknowledgements

References

1 (*a*) Y. Tanabe and Y. Nishibayashi, *Chem. Soc. Rev.*, 2021, **50**, 5201–5242; (*b*) Y. Tanabe and Y. Nishibayashi, *Coord. Chem. Rev.*, 2022, **472**, 214783; (*c*) *Transition Metal–Dinitrogen Complexes: Preparation and Reactivity*, ed. Y. Nishibayashi, Wiley-VCH, Weinheim, 2019.

2 M. J. Chalkley, M. W. Drover and J. C. Peters, *Chem. Rev.*, 2020, **120**, 5582–5636.

3 (*a*) Y. Ashida, K. Arashiba, K. Nakajima and Y. Nishibayashi, *Nature*, 2019, **568**, 536–540; (*b*) N. G. Boekell and R. A. Flowers II, *Chem. Rev.*, 2022, **122**, 13447–13477; (*c*) E. A. Boyd and J. C. Peters, *J. Am. Chem. Soc.*, 2022, **144**, 21337–21346.

4 Y. Ashida, T. Mizushima, K. Arashiba, A. Egi, H. Tanaka, K. Yoshizawa and Y. Nishibayashi, *Nat. Synth.*, 2023, **2**, 635–644.

5 C. Van Stappen, L. Decamps, G. E. Cutsail III, R. Bjornsson, J. T. Henthorn, J. A. Birrell and S. DeBeer, *Chem. Rev.*, 2020, **120**, 5005–5081.

6 C. M. Goodwin, P. Lömker, D. Degerman, B. Davies, M. Shipilin, F. Garcia-Martinez, S. Koroidov, J. Katja Mathiesen, R. Rameshan, G. L. S. Rodrigues, C. Schlueter, P. Amann and A. Nilsson, *Nature*, 2024, **625**, 282–286.

7 J. Chatt, A. J. Pearman and R. L. Richards, *Nature*, 1975, **253**, 39–40.

8 (*a*) F. A. Darani, G. P. A. Yap and K. H. Theopold, *Organometallics*, 2023, **42**, 1324–1330; (*b*) S. J. K. Forrest, B. Schluschass, E. Y. Yuzik-Klimova and S. Schneider, *Chem. Rev.*, 2021, **121**, 6522–6587; (*c*) C. E. Laplaza and C. C. Cummins, *Science*, 1995, **268**, 861–863.

9 A. Katayama, T. Ohta, Y. Wasada-Tsutsui, T. Inomata, T. Ozawa, T. Ogura and H. Masuda, *Angew. Chem., Int. Ed.*, 2019, **58**, 11279–11284.

10 (*a*) S. Kim, Y. Park, J. Kim, T. P. Pabst and P. J. Chirik, *Nat. Synth.*, 2022, **1**, 297–303; (*b*) M. T. Mock, *Nat. Synth.*, 2022, **1**, 262–263.

11 P. Garrido-Barros, J. Derosa, M. J. Chalkley and J. C. Peters, *Nature*, 2022, **609**, 71–76.

12 Y. Ashida, K. Arashiba, H. Tanaka, A. Egi, K. Nakajima, K. Yoshizawa and Y. Nishibayashi, *Inorg. Chem.*, 2019, **58**, 8927–8932.

13 (*a*) A. J. Kendall and M. T. Mock, *Eur. J. Inorg. Chem.*, 2020, 1358–1375; (*b*) M. T. Mock, S. Chen, R. Rousseau, M. J. O'Hagan, W. G. Dougherty, W. S. Kassel, D. L. DuBois and R. M. Bullock, *Chem. Commun.*, 2011, **47**, 12212–12214; (*c*) M. T. Mock, S. Chen, M. O'Hagan, R. Rousseau, W. G. Dougherty, W. S. Kassel and R. M. Bullock, *J. Am. Chem. Soc.*, 2013, **135**, 11493–11496; (*d*) M. Fritz, S. Demeshko, C. Würtele, M. Finger and S. Schneider, *Eur. J. Inorg. Chem.*, 2023, **26**, e202300011; (*e*) W. H. Monillas, G. P. A. Yap, L. A. MacAdams and K. H. Theopold, *J. Am. Chem. Soc.*, 2007, **129**, 8090–8091; (*f*) W. H. Monillas, G. P. A. Yap and K. H. Theopold, *Inorg. Chim. Acta*, 2011, **369**, 103–119; (*g*) X. Wang, Y. Wang, Y. Wu, G. X. Wang, J. Wei and Z. Xi, *Inorg. Chem.*, 2023, **62**,

18641–18648; (h) M. T. Mock, A. W. Pierpont, J. D. Egbert, M. O'Hagan, S. Chen, R. M. Bullock, W. G. Dougherty, W. S. Kassel and R. Rousseau, *Inorg. Chem.*, 2015, **54**, 4827–4839; (i) J. D. Egbert, M. O'Hagan, E. S. Wiedner, R. M. Bullock, N. A. Piro, W. S. Kassel and M. T. Mock, *Chem. Commun.*, 2016, **52**, 9343–9346; (j) I. Vidyaratne, J. Scott, S. Gambarotta and P. H. M. Budzelaar, *Inorg. Chem.*, 2007, **46**, 7040–7049.

14 (a) J. Yin, J. Li, G. X. Wang, Z. B. Yin, W. X. Zhang and Z. Xi, *J. Am. Chem. Soc.*, 2019, **141**, 4241–4247; (b) G. X. Wang, X. Wang, Y. Jiang, W. Chen, C. Shan, P. Zhang, J. Wei, S. Ye and Z. Xi, *J. Am. Chem. Soc.*, 2023, **145**, 9746–9754; (c) G. X. Wang, Z. B. Yin, J. Wei and Z. Xi, *Acc. Chem. Res.*, 2023, **56**, 3211–3222; (d) Z. B. Yin, B. Wu, G. X. Wang, J. Wei and Z. Xi, *J. Am. Chem. Soc.*, 2023, **145**, 7065–7070; (e) T. Shima, J. Yang, G. Luo, Y. Luo and Z. Hou, *J. Am. Chem. Soc.*, 2020, **142**, 9007–9016; (f) Y. Kokubo, K. Tsuzuki, H. Sugiura, S. Yomura, Y. Wasada-Tsutsui, T. Ozawa, S. Yanagisawa, M. Kubo, T. Takeyama, T. Yamaguchi, Y. Shimazaki, S. Kugimiya, H. Masuda and Y. Kajita, *Inorg. Chem.*, 2023, **62**, 5320–5333.

15 (a) A. J. Kendall, S. I. Johnson, R. M. Bullock and M. T. Mock, *J. Am. Chem. Soc.*, 2018, **140**, 2528–2536; (b) M. C. Eaton, B. J. Knight, V. J. Catalano and L. J. Murray, *Eur. J. Inorg. Chem.*, 2020, 1519–1524; (c) J. Li, J. Yin, G. X. Wang, Z. B. Yin, W. X. Zhang and Z. Xi, *Chem. Commun.*, 2019, **55**, 9641–9644.

16 Y. Ashida, A. Egi, K. Arashiba, H. Tanaka, T. Mitsumoto, S. Kuriyama, K. Yoshizawa and Y. Nishibayashi, *Chem. – Eur. J.*, 2022, **28**, e202200557.

17 (a) G. S. Girolami, J. E. Salt, G. Wilkinson, M. Thornton-Pett and M. B. Hursthouse, *J. Am. Chem. Soc.*, 1983, **105**, 5954–5956; (b) J. E. Salt, G. S. Girolami, G. Wilkinson, M. Motevalli, M. Thornton-Pett and M. B. Hursthouse, *J. Chem. Soc., Dalton Trans.*, 1985, 685–692.

18 D. M. Halepoto, D. G. L. Holt, L. F. Larkworthy, G. J. Leigh, D. C. Povey and G. W. Smith, *J. Chem. Soc., Chem. Commun.*, 1989, 1322–1323.

19 Structural metrics from XRD data of 2 collected here at 100 K. Data from ref. 17 at 295 K.

20 (a) M. L. Kuhlman and R. A. Flowers II, *Tetrahedron Lett.*, 2000, **41**, 8049–8052; (b) R. J. Enemærke, K. Daasbjerg and T. Skrydstrup, *Chem. Commun.*, 1999, 343–344.

21 J. E. Salt, G. Wilkinson, M. Motevalli and M. B. Hursthouse, *J. Chem. Soc., Dalton Trans.*, 1986, 1141–1154.

22 (a) J. Rittle and J. C. Peters, *J. Am. Chem. Soc.*, 2016, **138**, 4243–4248; (b) N. B. Thompson, P. H. Oyala, H. T. Dong, M. J. Chalkley, J. Zhao, E. E. Alp, M. Hu, N. Lehnert and J. C. Peters, *Inorg. Chem.*, 2019, **58**, 3535–3549.